Modeling Frequency Response Dynamics in Power System Scheduling

Ziyang Zhang*‡, Ershun Du*‡, Guiping Zhu*, Ning Zhang*‡,
Chongqing Kang*‡ and Minhui Qian§, João P. S. Catalão†
* Department of Electrical Engineering, Tsinghua University, Beijing, China
§ China Electric Power Research Institute (CEPRI), Nanjing, China
† Faculty of Engineering of the University of Porto (FEUP) and INESC TEC, Porto Portugal
‡ International Joint Laboratory on Low Carbon Clean Energy Innovation

***Abstract*—Since wind turbines or photovoltaic (PV) panels are generally connected to the power grid by power electronic inverters, the power system inertia is gradually decreasing along with the growing share of renewable energy. This jeopardizes the system frequency response dynamics so that the corresponding frequency security issue is becoming the bottle-neck factor that restricts the development of high renewable energy penetration. Consequently, power system scheduling models need to incorporate frequency dynamics. The difficulty lies in how to formulate the frequency security constraints from the perspective of hourly load-generation balance since the frequency dynamics have a shorter time scale (5~30s). Several modeling methods have been proposed based on different assumptions and simplifications. However, their accuracy is not clear. We first propose a novel method to formulate linear frequency security constraints, which considers more details of frequency response dynamics. Then, an evaluation methodology is designed to quantify the accuracy of those frequency constraints. Using this evaluation method, we compare two typical methods in recent literature with the proposed method. The results show the effectiveness and superiority of our proposed method.**

***Index Terms*--Frequency dynamics, frequency security constraints, high share of renewable energy, low inertia, power system scheduling.**

NOMENCLATURE

i	Index of generators
j	Index of piecewise subspaces
t	Time from contingency
Δf	Frequency deviation
H	System synchronous inertia
D	Load damping rate
ΔP_m	Power output adjustment of generators
ΔP_e	Power imbalance caused by contingency
f_{nadir}	Frequency nadir after contingency
R	Droop factor of the governor
F	Power fraction from the high-pressure turbine
K	Mechanical power gain factor
T	Reheat time constant
C_M	Ramp rate of generators after contingency
P	Scheduled output of the generator
Cap	Capacity of the generator
C_{NAD}	Overall system ramp rate after contingency
f_0	Rated frequency of power systems
$f_{\min}$	Secure threshold of system frequency
ΔP_{set}	Power imbalance caused by contingency
C_{MIN}	Required overall system ramp rate
FR	Maximum frequency reserve provided by the generator before frequency nadir (in LFSC model)
FR_{sys}	System overall frequency reserve (in IDFR model)
L_{total}	System overall load demand
T_d	Time that system delivers the frequency reserve
k^*	Lower bound of the product of system inertia and system overall reserve (the unique solution of (17))
ω_n	Natural oscillation frequency of frequency variations
ζ	Damping ratio of frequency variations
ω_r	Damped frequency of frequency variations
α	Amplitude coefficient of frequency variations
φ	Initial phase of frequency variations
ΔP	Frequency security margin
u_i	Binary parameter indicating whether generator participates in the frequency control
$\beta_j^C, \beta_j^H, \beta_j^F, \beta_j^R$	Piecewise linearization coefficients in FSM method

This work was supported in part by the National Key R&D Program of China (No. 2016YFB0900100), the National Natural Science Foundation of China (No. 51907100, 51677096). Also, J.P.S. Catalão acknowledges the support by FEDER funds through COMPETE 2020 and by Portuguese funds through FCT, under POCI-01-0145-FEDER-029803 (02/SAICT/2017).
Corresponding authors: Ning Zhang (ningzhang@tsinghua.edu.cn) and Chongqing Kang (cqkang@tsinghua.edu.cn).

I. INTRODUCTION

Since wind turbines or photovoltaic panels are generally connected to the power grid through power electronic inverters, power system inertia is gradually decreasing along with the growing share of renewable energy. High penetration of renewable energy integration would jeopardize the frequency

response dynamics of the power system and bring significant challenges to power system operation and security [1], [2]. The reasons are threefold. Firstly, low synchronous inertia leads to a faster frequency drop under contingency. Secondly, the considerable uncertainty and intermittency of renewable energy generation significantly increase the risk of the load-generation imbalance in the real-time operation of power systems. Furthermore, the frequency reserve is also becoming scarce as more dispatchable thermal generators are replaced by uncontrollable renewable energy generations [3]. Consequently, the frequency security issue is gradually becoming one of the bottle-neck factors that restrict the development of high renewable energy penetration [4]. For example, recently, Great Britain's electricity system suffered from a serious blackout on August 9, 2019. The inducement was a failure of two fossil fuel generators and one wind farm. Since almost 50% of total electricity was generated by wind power at that time, the failure dropped the frequency quickly and finally led to the frequency collapse [5]. This trend raises the need for considering frequency dynamics and imposing frequency security constraints into power system scheduling.

The difficulty lies in how to formulate frequency security constraints. Generally, power system scheduling focuses on the hourly load-generation balance, while the frequency dynamics has a shorter time scale (5~30s). The system frequency response (SFR) model based on the rotor swing equation is widely applied to describe the frequency response dynamics [6]. The SFR model contains a series of differential equations, and the frequency security requires to estimate the frequency nadir under contingency to judge whether the frequency is always above a secure threshold. From the perspective of power system scheduling, the generation schedule is supposed to keep enough synchronous inertia or frequency reserve for ensuring the frequency stability. The key to implementing this is to formulate the relationship between the system online inertia and the frequency reserve.

Several methods have been proposed in recent literature. Restrepo *et al.* consider the quasi-steady frequency limit in the unit commitment model to ensure the adequacy of frequency regulation reserve [7]. However, this model does not consider the frequency nadir which is generally much lower than the quasi-steady frequency under contingency. Chavez *et al.* simplify the governor characteristics of the generator, neglect the effect of load damping, and then deduce a simple analytical expression of frequency dynamics [8]. Based on this, linear frequency security constraints (LFSC) are introduced and incorporated into the optimal power flow model. Teng *et al.* also simplify the governor characteristics but consider the load damping effect in modeling the frequency dynamics, and then deduce the inertia-dependent frequency reserve (IDFR) constraints [9]. Different from those, Ahmadi *et al.* deduce the analytical formulation of the frequency nadir based on the SFR model ignoring the effect of load damping and then piecewise linearize the expression [10].

The urgent requirements for frequency security motivate more resources to provide frequency support, such as energy storage, demand-side, or even heat system. Their collaborative scheduling with the power system can also be optimized by introducing their frequency response model in the frequency security constraints. Based on the LFSC model, Wen *et al.* evaluate the benefits of the fast frequency response provided by battery energy storage in maintaining frequency security [11]. Under the framework of IDFR, Trovato *et al.* propose an optimal scheduling model of energy consumption and frequency response provision of thermostatically controlled loads[12], and Zhang *et al.* evaluate the benefits of integrated power and heat system on frequency security [13]. The renewable curtailment can be reduced when the thermal energy storage provides ancillary services [14]. Furthermore, the frequency security issue has also been explored in terms of the electricity market. Ela *et al.* discuss the motivation of introducing primary frequency response ancillary into the electricity market [15]. Zhang *et al.* study the market scheduling and pricing for primary and secondary frequency reserve [16]. Rayati *et al.* explore the Nash equilibrium of the frequency security constrained electricity market [17].

In summary, several innovative methods are available. Since the solution of frequency after contingency is a high order nonlinear problem, some assumptions and simplifications on the frequency response model are necessary to be formulated as frequency security constraints. The different simplifications raise the question of how is the performance of each method and which one is the best to be selected for different power systems. In order to address this issue, we propose an evaluation methodology to quantify the accuracy of those frequency security constraints. Furthermore, we also propose a novel method based on the frequency security margin (FSM) to formulate linear frequency security constraints, which consider the frequency response model more detailly. Based on the proposed evaluation method, we compare the proposed FSM method with two typical methods, namely LFSC in [8] and IDFR in [9]. The results of a case study show the effectiveness and superiority of our proposed FSM method.

The major contributions are summarized as follows. 1) we propose an evaluation methodology to quantify the accuracy of the frequency security constraints. 2) we formulate a novel FSM based frequency security constraints considering more details of the SFR model 3) We compare the performance of the proposed FSM method with two commonly used methods.

The remainder of this paper is organized as follows. Section II describes the methods of modeling frequency dynamics. Section III introduces the evaluation methodology. Section IV compares the performance of three models based on the evaluation methodology. Section V draws conclusions.

II. Modeling Frequency Dynamics

A. Framework

In this section, we firstly introduce the swing-equation based SFR model, which is widely applied to describe the frequency dynamics in the time scale of 0~30s. Then, three simplified methods are introduced to formulate frequency security constraints from the perspective of power system scheduling, namely the LFSC method, the IDFR method, and

the proposed FSM method. At the end of this section, a brief comparison of the three methods is provided.

B. Modeling Frequency Dynamics --- SFR Model

Generally, the system frequency dynamics can be captured by the rotor swing equation,

$$2H\frac{d\Delta f(t)}{dt}+D\Delta f(t)=\sum_i \Delta P_{mi}(t)-\Delta P_e(t) \qquad (1)$$

This differential equation demonstrates the relationship between the frequency derivation and generation-load power imbalance.

The system frequency response takes effect immediately after the power imbalance occurs. During the initial period, generators' governors are yet to respond because of the frequency dead band. The system frequency drops very rapidly, especially in a low-inertia system. When the frequency deviation exceeds the dead band, the governors start to adjust the output of the prime mover so that the frequency is gradually pulled back to a quasi-steady state. This process can be described using a multi-machine SFR model (MM-SFR), as shown in Fig. 1. The characteristic of governors is expressed as a first-order inertia element in this model. The limiters are added in this model to reflect the reserve spaces of each generator.

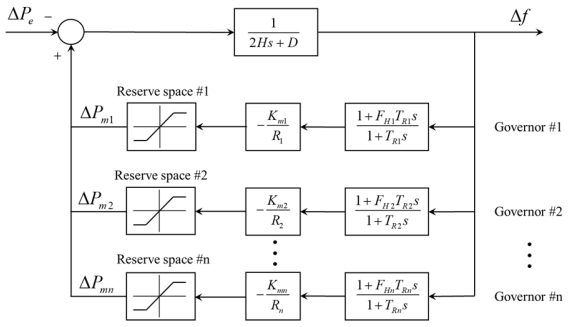

Figure 1. Multi-machine system frequency response model

The frequency nadir usually occurs in this primary frequency response process. It should be noted that the value of the quasi-steady frequency has deviations from that of the nominal frequency value. The frequency security requires the frequency nadir f_{nadir} above a secure threshold $f_{\min}$. However, in the power system scheduling problem, it is hard to directly obtain the frequency security constraints based on the SFR model due to its nonlinear and high-order feature. Simplifications are required for the SFR model to reformulate the frequency security constraints.

C. Method I --- LFSC Model

An intuitive method is to open the loop in Fig.1 with a simplified governor regulation characteristic [18]. It is assumed that the generator increases its output power with a constant ramp rate C_M, i.e.

$$\Delta P_m(t)=\begin{cases} C_M(t-t_0) & 0\le t<T_d \\ Cap-P & t\ge T_d \end{cases} \qquad (2)$$

where T_d equals $(Cap-P)/C_M$.

If the overall system ramp rate C_{NAD} is assumed constant, namely $\sum_i \Delta P_{mi}(t)=C_{NAD}t$, and the load damping effect is neglected, namely $D=0$, the system frequency dynamics can be depicted by:

$$2H\frac{d\Delta f(t)}{dt}=C_{NAD}t-\Delta P_e(t) \qquad (3)$$

where $\Delta P_e(t)=\Delta P_{set}u(t)$, ΔP_{set} is the power unbalance caused by the contingency, and $u(t)$ is the unit step function.

The time when the frequency nadir occurs, t_{nadir}, satisfies:

$$\Delta P_{set}=C_{NAD}t_{nadir} \qquad (4)$$

Then, the frequency nadir can be analytically formulated:

$$f_{nadir}=f_0-\frac{1}{4H}\frac{\Delta P_{set}^{\ 2}}{C_{NAD}} \qquad (5)$$

Obviously, frequency nadir f_{nadir} is a monotonically increasing function of the system equivalent ramp C_{NAD}. In order to keep the frequency always above the pre-defined secure threshold $f_{\min}$, C_{NAD} has a lower bound C_{MIN}.

$$C_{NAD}\ge C_{MIN}=\frac{1}{4H}\frac{\Delta P_{set}^{\ 2}}{f_0-f_{\min}} \qquad (6)$$

Consequently, t_{nadir} satisfies

$$t_{nadir}\le \Delta P_{set}/C_{MIN}=4H(f_0-f_{\min})/\Delta P_{set} \qquad (7)$$

Frequency security constraints are introduced as follows.

$$\sum_{i=1}^{n} FR_i\ge \Delta P_{set} \qquad (8)$$

$$FR_i\le 4C_{Mi}H(f_0-f_{\min})/\Delta P_{set} \qquad (9)$$

$$FR_i\le Cap_i-P_i \qquad (10)$$

$$H=\frac{1}{L_{total}}\sum_{i=1}^{n} H_i Cap_i x_i \qquad (11)$$

Constraint (8) represents that the sum of frequency reserve from all generators should be greater the system power imbalance. Constraints (9) and (10) limits the upper bound of FR_i. Constraint (11) calculates the system inertia according to the operation status of generators.

It should be noted that the frequency security constraints (8) to (11) are linear with respect to decision variables x_i and P_i. Thus, this method is named the linear frequency security

constraints (LFSC) model in this paper and has been widely applied in recent literature.

D. Method II --- IDFR Model

Ref. [9] assumes that the frequency reserve is delivered within T_d (10s, for example) and with a constant ramp rate following the contingency. Thus,

$$\sum_i \Delta P_{mi}(t) = FR_{sys} t / T_d \tag{12}$$

Consequently, according to (1), the frequency nadir can be analytically calculated as:

$$f_{nadir} = f_0 - \frac{\Delta P_{set}}{D} - \frac{2H \bullet FR_{sys}}{D^2 T_d} \ln\left(\frac{2H \bullet FR_{sys}}{DT_d \Delta P_{set} + 2H \bullet FR_{sys}}\right) \tag{13}$$

It can be proved that f_{nadir} is monotonically increasing with the univariate function $H \bullet FR_{sys}$. Therefore, the system frequency security requires:

$$H \bullet FR_{sys} \geq k^* \tag{14}$$

$$FR_{sys} \leq \sum_i \left(Cap_i - P_i\right) \tag{15}$$

$$H = \frac{1}{L_{total}} \sum_{i=1}^{n} H_i Cap_i x_i \tag{16}$$

where k^* is the unique solution to the following equation:

$$f_{\min} = f_0 - \frac{\Delta P_{set}}{D} - \frac{2k^*}{D^2 T_d} \ln\left(\frac{2k^*}{DT_d \Delta P_{set} + 2k^*}\right) \tag{17}$$

The frequency security constraints (14) to (16) describe the relationship between the system online inertia and the frequency reserve. Obviously, the frequency reserve requirement is dependent on the system inertia. More frequency reserve is required in a lower inertia system. Thus, this method is named the inertia-dependent frequency reserve (IDFR) model in this paper.

Although (14) has the nonlinear term $H \bullet FR_{sys}$, it can be linearized with the big M method with the auxiliary variables A_i representing $x_i FR_{sys}$.

$$\begin{gathered} \frac{1}{L_{total}} \sum_{i=1}^{n} H_i Cap_i A_i \geq k^* \\ FR_{sys} \leq \sum_i \left(Cap_i - P_i\right) \\ 0 \leq A_i \leq x_i M \\ FR_{sys} + \left(x_i - 1\right) M \leq A_i \leq FR_{sys} \end{gathered} \tag{18}$$

E. Method III --- FSM Model

Instead of simplifying the governor characteristic, the aggregate system frequency response (ASFR) model [19], shown in Fig.2, is utilized. All feedback paths are represented by a single aggregated governor.

Subsequently, the frequency nadir can be analytically derived. The detail derivation can be referred to in [19].

$$f_{nadir} = f_0 - \frac{R\Delta P_{set}}{DR+1}\left[1 + \sqrt{1-\zeta^2}\,\alpha e^{-\zeta \omega_n t_{nadir}}\right] \tag{19}$$

where

$$\begin{cases} \omega_n^{\,2} = \dfrac{DR+1}{2HRT_R}, \omega_r = \omega_n \sqrt{1-\zeta^2} \\ \zeta = \dfrac{DRT_R + 2HR + F_H T_R}{2\left(DR+1\right)} \omega_n \\ \alpha = \sqrt{\dfrac{1 - 2T_R \zeta \omega_n + T_R^2 \omega_R^2}{1-\zeta^2}} \\ t_{nadir} = \dfrac{1}{\omega_r} \tan^{-1}\left(\dfrac{\omega_r T_R}{\zeta \omega_r T_R - 1}\right) \end{cases} \tag{20}$$

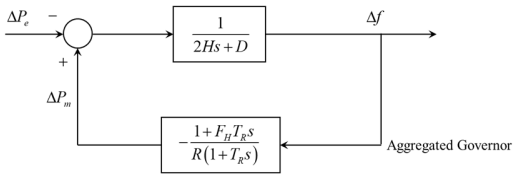

Figure 2. Aggregate system frequency response model

According to (18), the maximum frequency derivation $f_0 - f_{nadir}$ is proportional to ΔP_{set} . Hence, the frequency security constraints can be imposed on the size of ΔP_{set} . The maximum tolerable power imbalance within frequency security, namely the frequency security margin $\overline{\Delta P}$, is calculated as:

$$\overline{\Delta P} = \left(f_0 - f_{\min}\right) \bullet \frac{DR+1}{R\left(1 + \sqrt{1-\zeta^2}\,\alpha e^{-\zeta \omega_n t_{nadir}}\right)} \tag{21}$$

Subsequently, frequency security constraints are introduced as follows.

$$\overline{\Delta P} \geq \Delta P_{set} \tag{22}$$

$$H = \frac{1}{L_{total}} \sum_{i=1}^{n} H_i Cap_i x_i \tag{23}$$

$$\frac{1}{R} = \frac{1}{L_{total}} \sum_{i=1}^{n} \frac{K_{mi}}{R_i} Cap_i u_i \tag{24}$$

$$\frac{F_H}{R} = \frac{1}{L_{total}} \sum_{i=1}^{n} \frac{K_{mi} F_{Hi}}{R_i} Cap_i u_i \tag{25}$$

$$u_i \leq x_i \quad u_i, x_i \in \{0,1\} \tag{26}$$

$$Cap_i - P_i \geq \frac{u_i Cap_i K_{mi} / R_i}{\sum_j u_i Cap_i K_{mi} / R_i} \Delta P_{set} \tag{27}$$

Constraint (22) requires the FSM higher than the power imbalance under contingency. Constraints (23)-(25) calculate the parameters of the aggregated governor, according to the operation status of generators. x_i indicates whether the generator i is online. u_i indicates whether generator i participates in the frequency control. Constraint (26) denotes that only online generators can participate in frequency control. Constraint (27) indicates that the generators participating in frequency control should have sufficient reserve space. The frequency reserve quota for each generator is determined according to its droop damping factor.

Since equation (21) is nonlinear, constraint (22) is also nonlinear. The piecewise linearization (PWL) method is applied to linearize the constraint (22). Firstly, we divide the feasible domain into a series of subspaces $S_j\left(j=1,2,\cdots,N_J\right)$. Secondly, we search the closest hyperplane to approximate the constraint (21), namely:

$$\left(f_0-f_{\min}\right)\left(\beta_j^C+\beta_j^H H+\beta_j^F\frac{F_H}{R}+\beta_j^{\frac{1}{R}}\frac{1}{R}\right)\geq\Delta P_{set},\quad\forall j \tag{28}$$

where the coefficients $\beta_j^C,\beta_j^H,\beta_j^F,\beta_j^R$ can be obtained by solving the following optimization model.

$$\begin{aligned}&\max\ \sum_{m\in S_j}\left(\beta_j^C+\beta_j^H H_m+\beta_j^F\frac{F_{Hm}}{R_m}+\beta_j^R\frac{1}{R_m}\right)\\&s.t.\ \ \frac{DR_m+1}{R_m\left(1+\sqrt{1-\zeta_m^{\,2}}\alpha_m e^{-\zeta\omega_{nm}t_{nadirm}}\right)}\geq\\&\qquad\left(\beta_j^C+\beta_j^H H_m+\beta_j^F\frac{F_{Hm}}{R_m}+\beta_j^R\frac{1}{R_m}\right)\quad,\forall m\in S_j\end{aligned} \tag{29}$$

It should be noted that constraint (27) is nonlinear. With introducing an auxiliary continuous variable F representing $\frac{\Delta P_{set}}{\sum_j u_i Cap_i K_{mi}/R_i}$, constraint (27) can be rewritten as (30). Then nonlinear terms are only $u_i F$ which can be linearized by big M method in (31) with B_i representing $u_i F$

$$\begin{aligned}&Cap_i-P_i\geq F\,u_i Cap_i K_{mi}/R_i\\&\Delta P_{set}=F\sum_j u_i Cap_i K_{mi}/R_i\end{aligned} \tag{30}$$

$$\begin{aligned}&Cap_i-P_i\geq B_i Cap_i K_{mi}/R_i\\&\Delta P_{set}=\sum_i B_i Cap_i K_{mi}/R_i\\&0\leq B_i\leq u_i M\\&F+\left(u_i-1\right)M\leq B_i\leq F\end{aligned} \tag{31}$$

In summary, constraints (23)-(26), (28), (31), formulate linear frequency security constraints. It is named FSM model in this paper.

F. Discussion

Table I compares the abovementioned three methods in terms of calculation requirements in the preprocess, the consideration of load damping and governor characteristic, and the relationship between the variable of the model and the ΔP_{set}. For the preprocess, the proposed FSM method needs to conduct the PWL for linearizing the frequency security constraints while the IDFR method needs to calculate the parameter $k*$ via solving nonlinear equations. Both the IDFR model and FSM model consider a simplified governor regulation characteristic that the generator increases its output power with a constant ramp rate, while the LFSC model does not consider the load damping effect. The FSM model considers both the load damping effect and a more precise governor regulation characteristic. Furthermore, the proposed FSM model is linear with respect to ΔP_{set}. This indicates that ΔP_{set} could also be a decision variable for considering various contingencies.

TABLE I. COMPARISON OF THE THREE METHODS

	LFSC	**IDFR**	**FSM**
Preprocess	none	calculate $k*$	PWL
Load damping	×	√	√
Governor characteristic	simplified	simplified	√
Regard to ΔP_{set}	nonlinear	nonlinear	linear

As the three methods all formulate linear frequency constraints, the three methods can be easily incorporated into the commonly used scheduling model, such as OPF or UC, similar to the model presented in [11][12][16]. Thus, we will not consider a specific model in this paper but focus on the quantification of the accuracy. All the modeling methods try to achieve a trade-off between the model simplification and computational efforts. We count up the additional decision variables and constraints in the UC model on IEEE RTS-79 system. The results are shown in TABLE II. LFSC model performs better in the computational complexity. Since more details are considered in the IDFR and FSM models, the two models make a compromise on the complexity.

TABLE II. THE COMPARISON OF THE COMPLEXITY OF APPLICATION IN SCHEDULING MODEL BASED ON RTS-79 SYSTEM

	Continuous variables	Binary variables	Constraints
LFSC	20	0	40
IDFR	20	0	78
FSM*	23	19	174

* The number of piecewise subspaces N_J is 56.

III. EVALUATION METHODOLOGY

A. Framework

In section II, three models are introduced to formulate the frequency security constraints. The operation status satisfying those constraints are regarded to be frequency secure, which means that the frequency under contingency should always be above the pre-defined threshold. However, this is not always

the case, since the simplification or linearization in each model will introduce approximation error. To address this issue, we propose an evaluation methodology to quantify the accuracy of each model.

The framework of the evaluation methodology is shown in Fig. 3. Firstly, generate enough operation statuses to cover all of the possible operating statuses. Secondly, evaluate the frequency security for each operation status based on the multi-machine SFR model. The result is denoted by a binary variable (1 means secure, 0 means insecure) and is used as the benchmark. Then, obtain the frequency security evaluation results for the LFSC model, the IDFR model, and the proposed FSM model, respectively. Finally, several indices are proposed and calculated to quantify the accuracy of each model with respect to the SFR model.

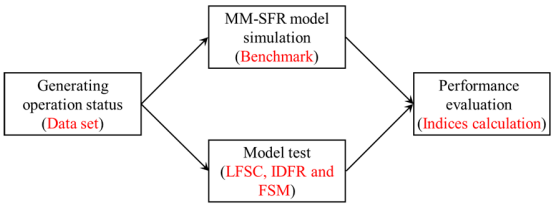

Figure 3. The framework of the evaluation methodology

B. Data Set

Since the frequency security constraints are mainly used in the power system scheduling problem, the data set should cover operation status over a whole year. To obtain enough data, we simulate the power system operation simulate on a modified IEEE RTS-79 test system [20] over a whole year with an hourly resolution using the software platform *Grid Optimization Planning Tool (GOPT)* developed by Tsinghua University [21]. The generation mix of the modified IEEE RTS-79 system is listed in Table II. The penetration of renewable energy generation is 28.62%.

TABLE III. COMPARISON OF THE THREE METHODS

Node	U155	U350	U76	U197	Wind	PV	Sum
B1	-	-	76*2	-	-	-	152
B3	-	-	76*2	-	-	-	152
B7	155*2	-	-	-	-	-	310
B13	-	-	-	197*3	340*2	160*2	1591
B14	-	-	-	-	340*2	160*3	1160
B15	-	-	76*2	-	340	-	492
B16	-	-	76*2	-	-	-	152
B18	-	350*2	-	-	-	-	700
B21	-	350	-	-	-	-	350
B22	-	350	-	-	-	-	350
B23	155*2		-	-	-	-	310
Total	620	1400	608	591	1700	800	5719

Fig. 4 illustrates the power system operation schedule over a week. The distribution of generated operation statuses is shown in Fig. 5. The X-axis and Y-axis represent the inertia and operating reserve of the entire system, respectively. The values of inertia and the reserves are distributed in a wide range due to the high penetration of renewable energy. The power imbalance ΔP_{set} imposed by contingency is set to 120 MW which is 4.2% of the peak load and 6.8% of the average load. The minimum secure frequency $f_{\min}$ is set to 49.5 Hz. Under these parameters, the numbers of secure and insecure operation statues are both sufficient to effectively demonstrate the performance of the three models.

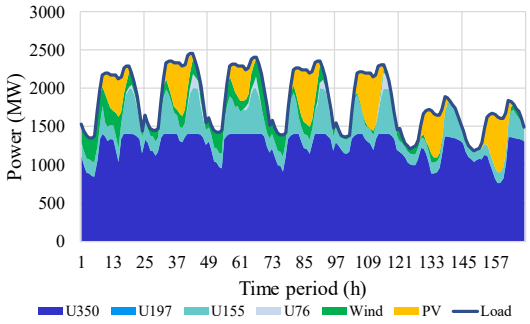

Figure 4. Simulating system operation result over a week

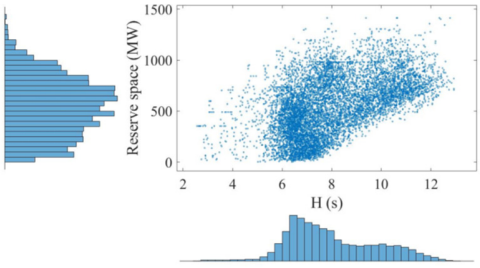

Figure 5. Distribution of system operation statuses

C. Evaluation Indices

For each operation status, the frequency security evaluation result for the test model can be classified into one of the four groups, namely true positive (TP), false positive (FP), false negative (FN), and true negative (TN). Table III shows the confusion matrix of binary classification, where the true condition is the benchmark result of the MM-SFR model, and predicted condition is the result of the test model. Four indices are introduced to evaluate the performance of the test model, including accuracy, recall, precision, and F1 scores. The calculation formulas are equations (32)-(35).

TABLE IV. CONFUSION MATRIX OF BINARY CLASSIFICATION

		True condition	
		1 (secure)	0 (insecure)
Predicted condition	1	True positive (TP)	False positive (FP)
	0	False negative (FN)	True negative (TN)

$$accuracy = \frac{num(TP) + num(TN)}{num(TP) + num(FP) + num(FN) + num(TN)} \quad (32)$$

$$recall = \frac{num(TP)}{num(TP) + num(FN)} \tag{33}$$

$$precision = \frac{num(TP)}{num(TP) + num(FP)} \tag{34}$$

$$F1 = \frac{2 \cdot precision \cdot recall}{precision + recall} \tag{35}$$

where $num(\bullet)$ is the number of system operation statuses belonging to the corresponding group.

The score of accuracy denotes the recognition rate of the test model. A higher accuracy score means a larger possibility of correct judgment. The recall score reflects the conservatism of the test model. A lower recall score means a larger possibility of evaluating secure status as insecurity. The precision score reflects the reliability of the test model. A higher precision score means higher reliability of the positive result. F1 score is the harmonic average of the recall and precision scores, which can reflect the general performance of the test model in conservatism and reliability.

IV. Result

A. Basic Results

Fig. 6 shows the frequency security evaluation results of different models. The blue points denote the secure operation status, while the red one indicates the insecure operation status. The boundary between secure and insecure operation status generally decreases along the X-axis. This demonstrates the fact that the power system with lower inertia requires more frequency reserves to undertake the same power imbalance. Nevertheless, the boundary is not only determined by reserve and system inertia since governor characteristics and load damping factors also have impacts on the boundary. Consequently, it is hard to give an analytical function to describe the relationship between the system inertia and the required frequency reserve.

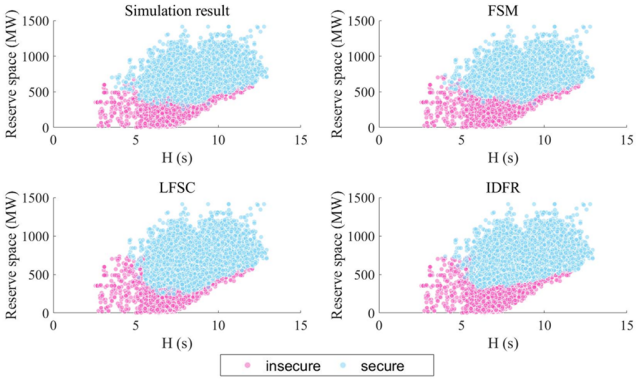

Figure 6. Frequency security evaluation results of different models

The quantitative evaluation indices are listed in Table IV. The results show that the proposed FSM model performs best in three models in terms of accuracy, precision and F1 score.

TABLE V. Evaluation Indices of the Three Models

	accuracy	recall	precision	F1
FSM	96.00%	92.87%	100.00%	96.30%
LFSC	91.13%	96.62%	88.58%	92.42%
IDFR	89.84%	94.76%	88.02%	91.27%

Fig. 7 clearly demonstrates the difference in evaluation results between the benchmark and the test model. The operation status is colored green if with the same evaluation result, colored purple if evaluating secure status to be insecure, and colored red if evaluating insecure status to be secure. Obviously, operation statuses with wrong evaluation are mainly distributed around the boundary between security and insecurity. Specifically, the secure operation statuses are more likely to be wrongly evaluated to be insecure when the system inertia is lower, and the insecure operation statuses are more likely to be wrongly evaluated to be secure when the system inertia is higher. As very few insecure statuses are wrongly judged as secure ones, FSM model is the most conservative but also the most reliable among the three models. The reasons are two-fold. 1) The linearization method (29) is conservative because $\overline{\Delta P}$ is lower than the real maximum tolerable power imbalance. 2) Constraint (27) guarantees the adequacy of frequency reserve.

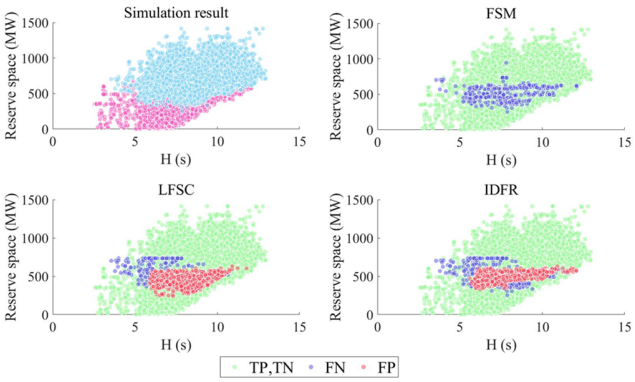

Figure 7. Model performance compared to simulation results

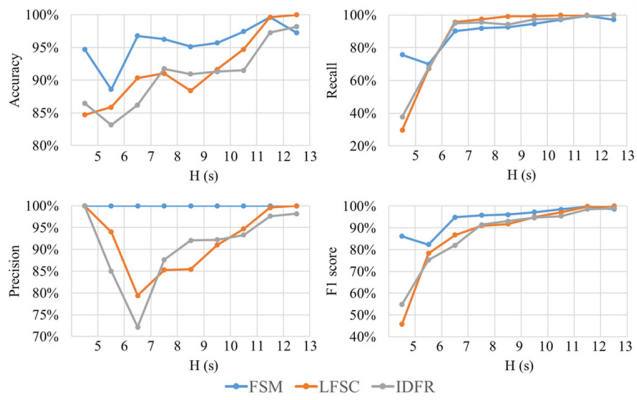

Figure 8. Evaluation indices under different system inertia

Fig. 8 shows the evaluation indices of the three models under different system inertia conditions. Overall, the proposed FSM model always performs better than the other two models. The accuracy of all the three models generally performs worse under lower system inertia condition. As for the model conservatism, the recall score of all the three models generally performs worse under lower system inertia condition. This verifies the fact that the secure operation statuses are more likely to be wrongly evaluated to be insecure when the system inertia is lower.

B. *Sensitivity Analysis*

In this part, we first evaluate the model performance to the share of renewable energy in power systems. Four cases with renewable penetration level from 19.8% to 41.7% by changing the installed capacity of renewable energy. The distribution of operation statuses under different renewable penetration levels is shown in Fig. 9. Generally, operation statuses under higher renewable penetration levels are more dispersed. Specifically, under a high renewable penetration level, the power system is more likely to be operated at the lower-left corner with low inertia and low reserve such that more system operation statuses are insecure.

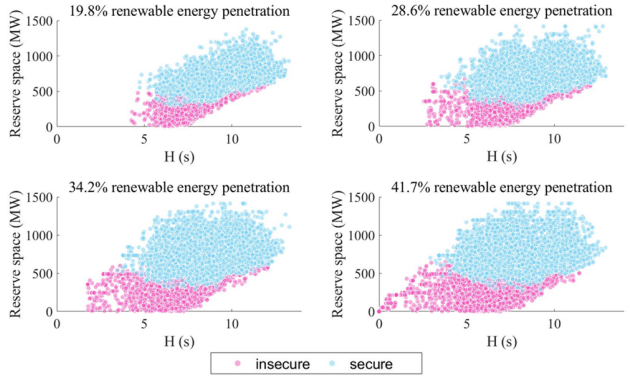

Figure 9. Distribution of system operation status under different renewable energy penetration levels

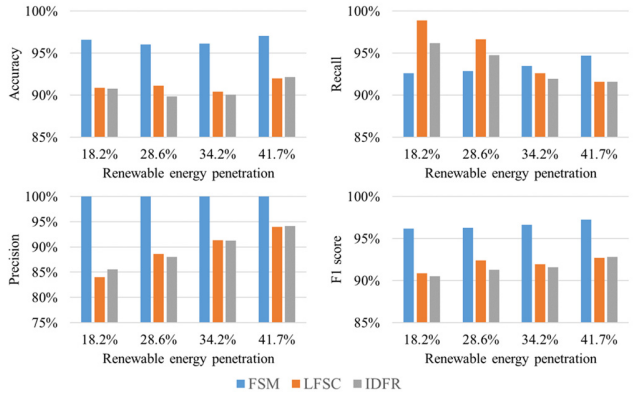

Figure 10. Evaluation indices under different renewable energy penetration

Fig. 10 shows the evaluation indices of the three models under different renewable penetration levels. In general, the proposed FSM always performs better in accuracy, precision and F1 score than the other two models under different renewable energy penetration levels, which demonstrates the superiority of the FSM method. The accuracy score of the FSM model remains almost the same (above 95%) because more details are considered, which suggests the robustness of the FSM model. The performances of the other two models are similar. However, the performances of LFSC model fluctuate more than those of IDFR model.

Since the characteristics of the simplified governor, C_M and T_d, can't be directly obtained from the MM-SFR model. In the above case studies, C_{Mi} and T_d are estimated according to the average value of 8760 operation statues. Fig. 11 compares the performance of LFSC and IDFR model under different simplified governor characteristics. As T_d increases or C_{Mi} decreases, the recall of the two models decreases while precision increases because the governor regulation ability is underestimated. The result also indicates the FSM model achieves a better trade-off between recall and precision than the two models. The curve of LFSC model is unsmooth, indicating that LFSC model is sensitive to the parameters C_M, which explain the larger fluctuations under different renewable energy shares.

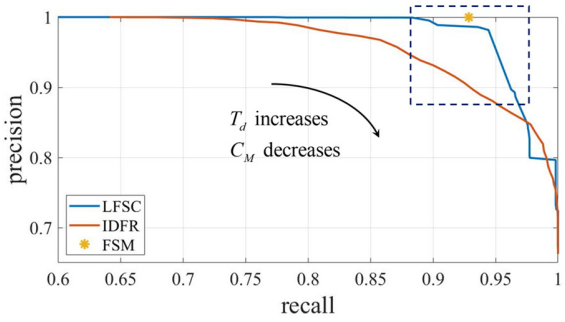

Figure 11. Performance of LSFC and IDFR model under different parameters

V. Conclusion

Frequency security is becoming one of the bottle-neck factors that restrict the development of high renewable energy penetration. It is essential to consider the system frequency dynamics and impose frequency security constraints on power system scheduling. This paper compares three methods that simplify the system frequency response model and formulates the frequency security constraints in a different way. The results show that the proposed FSM model performs better than the other two models proposed in recent literature, namely LFSC and IDFR, under different renewable energy penetration levels. The accuracy of the FSM model remains nearly the same and above 95% in all the situations, which demonstrates the effectiveness and robustness of the FSM model.

References

[1] P. Tielens and D. Van Hertem, "The relevance of inertia in power systems," Renewable and Sustainable Energy Reviews, vol. 55, pp. 999 - 1009, 2016.

[2] M. A. Ortega-Vazquez and D. S. Kirschen, "Assessing the Impact of Wind Power Generation on Operating Costs," in *IEEE Transactions on Smart Grid*, vol. 1, no. 3, pp. 295-301, Dec. 2010.

[3] M. Ghofrani, A. Arabali, M. Etezadi-Amoli and Y. Baghzouz, "Operating reserve requirements in a power system with dispersed wind generation," *2012 IEEE PES Innovative Smart Grid Technologies (ISGT)*, Washington, DC, 2012, pp. 1-8.

[4] E. V. M. Garrigle, J. P. Deane and P. G. Leahy, "How much wind energy will be curtailed on the 2020 Irish power system?" *Renewable Energy*, vol. 55, pp. 544 - 553, 2013.

[5] National Grid ESO, "Interim Report into the Low Frequency Demand Disconnection (LFDD) following Generator Trips and Frequency Excursion on 9 Aug 2019,",16 August 2019. [Online]. Available: https://www.nationalgrideso.com/document/151081/download

[6] P. M. Anderson and M. Mirheydar, "A low-order system frequency response model," *IEEE Transactions on Power Systems*, vol. 5, pp. 720-729, 1990-01-01 1990.

[7] J. F. Restrepo and F. D. Galiana, "Unit Commitment with Primary Frequency Regulation Constraints," *IEEE Transactions on Power Systems*, vol. 20, pp. 1836-1842, 2005.

[8] H. Chavez, R. Baldick, S. Sharma, "Governor Rate-Constrained OPF for Primary Frequency Control Adequacy". *IEEE Transactions on Power Systems*, vol.29, no.3, pp:1473-1480, 2014.

[9] F. Teng, V. Trovato and G. Strbac, "Stochastic Scheduling with Inertia-Dependent Fast Frequency Response Requirements," *IEEE Transactions on Power Systems*, vol. 31, pp. 1557-1566, 2016.

[10] H. Ahmadi and H. Ghasemi, "Security-Constrained Unit Commitment with Linearized System Frequency Limit Constraints," *IEEE Transactions on Power Systems*, vol. 29, pp. 1536-1545, 2014.

[11] Yunfeng Wen, Wenyuan Li, Gang Huang, Xuan Liu, "Frequency Dynamics Constrained Unit Commitment With Battery Energy Storage", *IEEE Transactions on Power Systems*, vol. 31, no. 6, pp. 5115-5125, 2016.

[12] Vincenzo Trovato, Fei Teng, Goran Strbac, "Role and Benefits of Flexible Thermostatically Controlled Loads in Future Low-Carbon Systems", *IEEE Transactions on Smart Grid*, vol. 9, no. 5, pp. 5067-5079, 2018.

[13] Xi Zhang, Goran Strbac, Nilay Shah, Fei Teng, Danny Pudjianto, "Whole-System Assessment of the Benefits of Integrated Electricity and Heat System", *IEEE Transactions on Smart Grid*, vol. 10, no. 1, pp. 1132-1145, 2019.

[14] P. Romanos, E. Voumvoulakis, C. N. Markides, and N. Hatziargyriou,"Thermal Energy Storage Contribution to the Economic Dispatch of Island Power Systems,"CSEE Journal of Power and Energy Systems, vol. 6, no. 1, pp. 100–110, Mar. 2020.

[15] E. Ela, V. Gevorgian, A. Tuohy, B. Kirby, M. Milligan and M. O'Malley, "Market Designs for the Primary Frequency Response Ancillary Service—Part I: Motivation and Design," in *IEEE Transactions on Power Systems*, vol. 29, no. 1, pp. 421-431, Jan. 2014.

[16] Guangyuan Zhang, Erik Ela, Qin Wang, "Market Scheduling and Pricing for Primary and Secondary Frequency Reserve", *IEEE Transactions on Power Systems*, vol. 34, no. 4, pp. 2914-2924, 2019.

[17] Mohammad Rayati, Mohammadreza Toulabi, Ali Mohammad Ranjbar, "Optimal Generalized Bayesian Nash Equilibrium of Frequency-Constrained Electricity Market in the Presence of Renewable Energy Sources", in *IEEE Transactions on Sustainable Energy*, vol. 11, no. 1, pp. 136-144, 2020.

[18] I. Egido, F. Fernandez-Bernal, P. Centeno and L. Rouco, "Maximum Frequency Deviation Calculation in Small Isolated Power Systems," in *IEEE Transactions on Power Systems*, vol. 24, no. 4, pp. 1731-1738, Nov. 2009.

[19] Q. Shi, F. Li and H. Cui, "Analytical Method to Aggregate Multi-Machine SFR Model With Applications in Power System Dynamic Studies," in *IEEE Transactions on Power Systems*, vol. 33, no. 6, pp. 6355-6367, Nov. 2018.

[20] Probability Methods Subcommittee, "IEEE Reliability Test System," *IEEE Trans. Power Apparatus and Systems*, vol. PAS-98, pp. 2047-2054,1979.

[21] "Power system planning decision-making and evaluation system GOPT technical manual," Department of Electrical Engineering, Tsinghua University, Beijing, 2010 (in Chinese).